Optical parameters of CaF_2, LiF, NaCl and KCl single crystals in the X-ray spectral range

[1]Raransky M.D., [1]Balazyuk V.N., [2]Sergeev V.M. and [1]Melnyk M.I.

[1]Yu. Fedkovych Chernivtsi National University, 2 Kotsyubynsky St., 58012 Chernivtsi, Ukraine, e-mail: ftt2010@bigmir.net
[2]G. Skovoroda Kharkiv National Pedagogical University, 29 Artem St., 61002 Kharkiv, Ukraine, e-mail: ser_vik@ukr.net

Received: 25.01.2011

Abstract

In this work, pendulum fringe and X-ray interferometry methods are used for measuring F_{hkl} parameter, atomic dispersion amplitudes f_a, dispersion corrections $\Delta f'$, and single decrements of refractive indices α for CaF_2, LiF, NaCl and KCl single crystals.

Keywords: single crystals, pendulum fringes, X-ray interferometry, structural dispersion parameters

PACS: 41.50.+h
UDC: 548.4:548.734

1. Introduction

Single crystals of alkali halides are widely applied in technologies of optical instrument engineering as elements of optical schemes, X- and γ-radiation scintillation detectors, thermo-luminescent dosimeters and colour centre lasers [1–2]. From the standpoint of X-ray diffraction, the above crystals are traditionally referred to typical representatives of ideally mosaic crystals [3–7]. However, advances in the technology of single crystal growth and X-ray topography methods have changed the conventional point of view. Acquisition of pendulum fringes appearing at X-ray diffraction from these single crystals has confirmed directly a possibility for growing perfect single crystals [8].

In this work, the methods of pendulum fringes and X-ray interferometry [8–12] have been used in order to measure structural (F_{hkl}) and atomic (f_a) dispersion amplitudes, as well as dispersion corrections ($\Delta f'$) and single decrements (α) of refractive indices. Our studies have been performed using single crystals of CaF_2, LiF, NaCl, and KCl grown from a melt along [100] direction. Topographic studies have shown that our single crystals have dislocation densities ~ 10^2 cm^{-2} and, moreover, a presence of mosaic blocks in NaCl and KCl could not be avoided completely. Linear X-ray absorption coefficients of these single crystals are low, making possible topographic investigations of rather thick crystals (~ 1 cm). Notice that the optical parameters F_{hkl}, f_a, $\Delta f'$ and α mentioned above facilitate predicting unambiguously resources for application of single crystals in the short-wave X-ray optics.

It should also be pointed out that the above optical parameters have earlier been measured by many authors using classical techniques, e.g. the methods of integral intensities of X-ray dispersion, deviation from the Bragg's law, and total external reflection. However, the corresponding measurement errors have been high enough (7–10% [3–5]). It is a high structural perfection of our CaF_2, LiF, NaCl and KCl single crystals that has allowed us to apply, for the first time, interferometry-precision research methods. So, the pendulum fringe method enables measuring the F_{hkl}, f_a and $\Delta f'$ values with the errors of 0.1–1.0%, while the X-ray interferometry yields the $\Delta f'$ and α values for any amorphous, polycrystalline or single-crystalline material, being characterised with the errors as low as 0.1–0.5% [8–12].

2. Experimental

Traditional methods for determining the F_{hkl} and f_a parameters are based on measuring the integral intensities of dispersion. Since the accuracy for the absolute values of integral intensities is low (7–10%), these methods have not gained wide acceptance. The pendulum fringe method [12] makes it possible to determine F_{hkl} and f_a without measuring the energy dispersion parameters. According to bidirectional approximation for dynamic scattering of X-rays, there are two coherent waves propagating towards each of reciprocal lattice nodes 0 and *m*, with the interference period [3–5] equal to

$$\Lambda_{(0,m)} = \frac{2\pi}{|\Delta K|} = \frac{(\gamma_0\gamma_m)^{1/2}}{C\dfrac{e^2\lambda}{mc^2\times\pi V}F_{hkl}}. \qquad (1)$$

Here the notation $|\Delta K| = \left|\vec{K}_{(0,m)_1} - \vec{K}_{(0,m)_2}\right|$ is used (with $\vec{K}_{(0,m)_1}$ and $\vec{K}_{(0,m)_2}$ being the wave vectors), γ_0 and γ_m are the direction cosines of the wave incident at a crystal and the diffracted wave, respectively, $C = \dfrac{1+\cos^2 2\theta}{2}$ denotes the polarisation factor, $\dfrac{e^2}{mc^2}$ the classical electron radius, V the unit cell volume, λ the wavelength, e and m respectively the charge and the mass of electron, c the free-space velocity, and θ the diffraction angle.

The structural amplitude F_{hkl} is as follows:

$$F_{hkl} = \sum_{a=1}^{N} f_a \exp[-2\pi i(hu + kv + lw)], \qquad (2)$$

where u, v, w are the coordinates of the unit cell base atoms, and h, k, l are Miller indices. Inverse proportionality between the pendulum oscillation periods Λ and the structural amplitude F_{hkl} enables measuring, with a high precision (~ 0.1–1%), the absolute values of the structural amplitude F_{hkl} and, hence, the atomic amplitudes f_a.

Single crystals were made in the shape of wedges, with the apex angles of 1–3 angular degrees. X-ray diffraction from different atomic planes (*hkl*) was achieved using CuK_α- and MoK_α-radiations. The pendulum oscillations of X-rays observed in the dif-

fracted beams were recorded on photoplates. The experimental procedures and the effect of different factors on the measurement accuracy have earlier been described in [12] and tested on dislocation-free Ge and Si single crystals. As an example, Fig. 1 illustrates the pendulum fringes seen in the case of CaF_2 single crystals. A presence of clear-cut images of the pendulum oscillations testifies to high structural perfection of our single crystals.

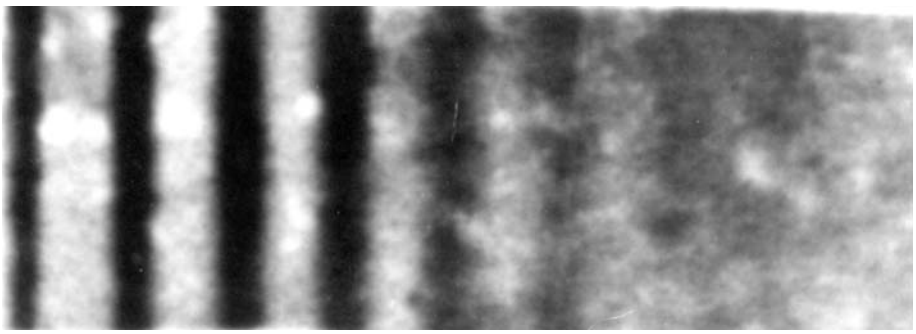

Fig. 1. Pendulum fringes observed in CaF_2 single crystals: (200) reflection, CuK_α-radiation.

3. Results and discussion

3.1. Structural and atomic dispersion amplitudes

The structural amplitude for the fluorite obtained for the reflection planes (*hkl*) characterised by an even sum of indices ($h + k + l = 2n$) is equal to a sum (or difference) of the atomic amplitudes of calcium (f_{Ca}) and fluorine (f_F). For any odd $h + k + l = 2n + 1$ value, the F_{hkl} factor represents a multiple of the calcium amplitude (f_{Ca}) [13]. Then one can determine separately the atomic dispersion amplitudes for the Ca and F atoms, following from the Λ periods.

Table 1. Structural and atomic amplitudes of CaF_2.

hkl	F_T^H	F_T^{DT}	F_e^P	$f_{T\,\mathrm{F}}^{DT}$	$f_{T\,\mathrm{Ca}}^{DT}$	$f_{e\,\mathrm{F}}^{P}$	$f_{e\,\mathrm{Ca}}^{P}$
111	60.40	62.17	60.30	7.41	15.541	–	15.11
220	93.80	96.96	96.03	5.72	12.785	5.92	12.37
311	45.60	46.52	44.17	5.05	11.63	–	11.04
222	8.00	6.78	7.70	4.81	11.32	4.38	10.68
321	8.42	7.32	8.60	4.46	10.74	3.98	10.02
400	72.11	74.37	77.10	4.16	10.27	4.6	10.18

Table 1 gathers the values of the structural amplitudes F_T^H calculated with the Hartree-Fock method and taken from [14], the amplitudes F_T^{DT} calculated with accounting for relativistic correction constants and taken from [15], along with the amplitudes F_e^P measured experimentally in this work basing on the pendulum fringe periods Λ. The

theoretical and experimental atomic dispersion amplitudes of Ca and F can also be analysed. Here the f_e^P(Ca) and f_e^P(F) parameters have been calculated from the experimental values F_e^P for different reflections (*hkl*). Dispersion corrections $\Delta f'$ and $\Delta f''$ taken from [14] have been introduced to the experimental F_e^P values (one has $\Delta f'_{\mathrm{Ca}} = 0.2$, $\Delta f''_{\mathrm{Ca}} = 0.4$, and $\Delta f'_{\mathrm{F}} = \Delta f''_{\mathrm{F}} = 0$ for the case of MoK_α-radiation). The spread between the experimental (F_e^P) and calculated (F_T^{DT}) values is 2–5%. In our case it would be necessary to take into account the contribution of both dispersion and temperature effects to the X-ray dispersion amplitudes. That will be done later, since the absence of reliable experimental values F_e in this work has hindered the more detailed analysis.

Table 2. Structural amplitudes of LiF.

hkl	F_T^H	F_T^{DT}	$F_e^{Z_1}$	$F_e^{Z_2}$	F_e^P
111	18.16	19.72	19.00	–	19.81
200	29.51	30.12	27.10	23.70	30.05
220	22.18	22.92	21.00	19.70	21.41
311	8.93	9.62	9.31	–	9.33
222	18.24	18.64	16.70	–	18.67
400	15.24	15.73	13.90	13.30	15.46

Table 2 represents both the theoretical and experimental structural amplitudes for the LiF single crystal using the notation assumed earlier. We have also analysed the values $F_e^{Z_1}$ and $F_e^{Z_2}$ obtained experimentally by Zachariasen [16] for spherical LiF samples, basing on the integral dispersion intensities for the MoK_α- and CuK_α-radiations, respectively. The F_e^P values listed in Table 2 account for both the dispersion and temperature corrections [8, 12]. Notice that $F_T^{DT} > F_T^H$. There is satisfactory agreement between the F_e^P and F_T^{DT} values (see Table 2). The values $F_e^{Z_{1,2}}$ are scattered by ~ 10% as compared to F_T^{DT} and F_e^P, which lies within the limits of experimental errors for the integral dispersion intensities [16].

Table 3 displays the structural amplitudes $F_{T,e}$ for the NaCl and KCl single crystals. The values F_e^P are given with the temperature and dispersion corrections taken from [14]: $\Delta f'_{Na} = 0.1$, $\Delta f''_{\mathrm{Na}} = 0.2$, $\Delta f'_{\mathrm{K}} = 0.3$, $\Delta f''_{\mathrm{K}} = 1.1$, $\Delta f'_{\mathrm{Cl}} = 0.3$, and $\Delta f''_{\mathrm{Cl}} = 0.7$. There is fair agreement between the experimental and theoretical structural amplitudes. At the same time, the errors for the structural amplitudes F_e^P has increased up to 2–5%, as a result of presence of different dislocations, stresses and block boundaries in the NaCl and KCl samples.

Table 3. Structural amplitudes of NaCl and KCl.

hkl	NaCl			KCl		
	F_T^H	F_T^{DT}	F_e^P	F_T^H	F_T^{DT}	F_e^P
111	19.09	18.57	20.01	5.72	5.68	6.04
200	85.15	85.82	86.45	113.82	113.83	111.51
220	72.28	72.79	74.07	97.14	97.27	92.72
311	11.39	10.66	13.68	6.57	6.51	6.87
222	63.64	64.81	63.82	86.60	86.66	89.05
400	58.27	59.15	62.46	79.25	79.35	77.14

3.2. Single decrements of refractive indices and dispersion corrections

It is well-known that the phase velocity v of electromagnetic wave propagating in crystal differs from the velocity c in vacuum. As a consequence, wave refraction takes place at the interface crystal–vacuum, with the appropriate index

$$n = \frac{c}{v} = 1 - \alpha - i\beta. \tag{3}$$

Here $\beta = \frac{\lambda}{4\pi}\mu$, where μ is the linear absorption coefficient. In the range of X-ray wavelengths, single crystals of CaF_2, LiF, NaCl and KCl can be considered as non-absorptive and so we have $n = 1 - \alpha$. The parameter α ($\alpha \approx 10^{-6}$) is called as a single decrement of the refractive index.

The atomic dispersion function f_a in a wide range of wavelengths is equal to [3–5]

$$f_a = \frac{\omega^2}{\left(\omega^2 - \omega_g^2 + i\gamma\omega\right)}, \tag{4}$$

where ω is the frequency of radiation incident at a crystal, ω_g the intrinsic frequency of atomic oscillations, and the coefficient γ equals to $\gamma = \frac{2}{3}\frac{e^2\omega}{c^3} \approx 10^{-7}$. Separating real and imaginary parts in Eq. (4) yields

$$f_a = f_0 + \Delta f' + i\Delta f'', \tag{5}$$

where the values $\Delta f'$ and $\Delta f''$ coincide respectively with α and β appearing in Eq. (3), within the accuracy of constant factors. Therefore, the X-ray refractive index n is determined in terms of the atomic dispersion function [3–5]:

$$n = 1 - \frac{N\lambda^2}{2\pi}\frac{e^2}{mc^2} f_a. \tag{6}$$

If $\omega \approx \omega_g$, there appear resonance effects resulting in abnormal absorption of X-rays. As shown by experimental investigations, the dispersion effects cannot be ignored completely even in the case of $\omega >> \omega_g$.

Classical methods for studying $n(\lambda)$ and $\Delta f'(\lambda)$ have essential drawbacks associated, e.g., with infinitesimal α values and inaccurate measurements of angles and integral intensities. As a result, the accuracy for those parameters is greatly reduced (down to 7–10% [3–5]). On the contrary, this study employs the pendulum fringe and the X-ray interferometry methods [8–12] related to interference pattern geometry, rather than measuring the energy parameters themselves, and so they enable n and $\Delta f'$ to be measured with much higher accuracy (~ 0.1–0.5%).

The pendulum fringe method accounts for the contribution of dispersion effects to the structural amplitude ($F_{hkl} \pm \Delta F_{hkl}$), resulting in a change of pendulum oscillation periods Λ given by Eq. (1). For the CaF_2 single crystals, we have used reflection of X-rays from the crystallographic planes (111). Then the dispersion corrections for the fluorine atoms can be ignored, since we have $\Delta f'_F = 0$ for both the CuK_α- and MoK_α-radiations [14]. Therefore, the pendulum fringe period for these cases may be assumed as a reference one. Moreover, the structural amplitude $F_{(111)}$ is determined only by the atomic amplitude of calcium, $F_{(111)} = 4f_{Ca}$.

Table 4. Dispersion corrections $\Delta f'$ for Ca in CaF_2 crystals.

λ, Å	$\Delta f'^{,B}_{Ca}$	$\Delta f'^{,C}_{Ca}$	$\Delta f'^{,P}_{Ca}$
0.70926	0.22	0.203	0.220
1.47634	–	–	0.324
1.5405	0.28	0.341	0.308
1.65784	0.23	–	0.290
1.78892	0.16	–	0.278
2.28962	–0.41	–0.201	–0.250

Table 4 represents the experimental values $\Delta f'^{,P}_{Ca}$ obtained for the CaF_2 crystals issuing from the pendulum fringe periods in the wavelength range of 0.7–2.2 Å. Notice that the absorption edge for Ca amounts to $\lambda_K = 3.0702$ Å [14]. For comparison, the calculated values $\Delta f'^{,B}_{Ca}$ [17] and $\Delta f'^{,C}_{Ca}$ [18] are also shown in Table 4. The experimental results $\Delta f'^{,P}_{Ca}$ agree well with the Cromer's theory [18], where the dispersion corrections $\Delta f'$ and $\Delta f''$ are calculated using the relativistic Dirac-Slater wave functions. We also emphasise that the pendulum fringe method provides determining the dispersion corrections separately for each sort of atoms in complex crystal lattices.

The X-ray interferometric method [8, 12] involves measuring an interference fringe shift due to a change in the optical path occurring in one of the interferometer arms upon introduction of a sample under study. The shift ΔN is related to the single decrement α of the refractive index via the relation

$$\alpha = 1 - n = \frac{\lambda \Delta N}{t} + (1 - n_a), \tag{7}$$

where t is the crystal thickness and n_a the refractive index of air. Fig. 2 illustrates a shift in the Moiré fringes observed after introduction of a wedge-shaped CaF_2 sample.

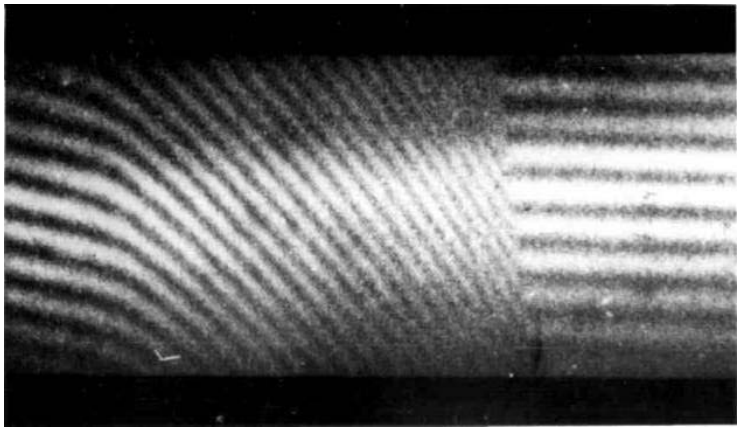

Fig. 2. Moiré fringe shift observed for the wedge-shaped CaF_2 sample using CuK_α - radiation.

In order to measure the parameters $\Delta f'$ and α for the CaF_2, NaCl and KCl single crystals, we have used K_α-radiations of Cu, Ni, Co, Fe and Cr anodes. Table 5 gives the values $\Delta f'^{,P}$ and α_e^P for those crystals, along with the values α_T^C calculated with the dispersion corrections for the individual atoms, according to Cromer [18].

Table 5. Dispersion corrections $\Delta f'$ and single decrements of refractive indices α for the crystals under study

λ, Å	CaF_2			NaCl			KCl		
	$\alpha_e^P, 10^{-6}$	$\Delta f_e'^P$	$\alpha_T^C, 10^{-6}$	$\alpha_e^P, 10^{-6}$	$\Delta f_e'^P$	$\alpha_T^C, 10^{-6}$	$\alpha_e^P, 10^{-6}$	$\Delta f_e'^P$	$\alpha_T^C, 10^{-6}$
1.5405	7.668	0.167	7.642	6.748	0.221	6.695	6.249	0.378	6.185
1.65784	8.875	0.149	8.830	7.821	0.243	7.154	7.236	0.309	7.163
1.78892	10.330	0.137	10.281	9.115	0.269	9.028	8.417	0.334	8.340
1.935997	12.090	0.120	12.041	10.683	0.291	10.573	9.854	0.302	9.767
2.28962	16.782	0.102	16.995	14.947	0.299	14.789	13.739	0.204	13.842

4. Conclusions

1. The atomic and structural amplitudes and the dispersion corrections are determined for the first time for the CaF_2, LiF, NaCl and KCl single crystals, using highly precise pendulum fringe and X-ray interferometry methods, with no direct measurements of the energy dispersion parameters.

2. Unlike the X-ray interferometry method, the pendulum fringe method has enabled measuring the f_a and $\Delta f'$ parameters separately for each atom in a chemical compound, as shown on the example of CaF_2 crystal (see Table 1).
3. The above methods may be successfully used in the range of X-ray wavelengths, even in the vicinity of *K*-edge of absorption, which is impossible in frame of the integral intensity method.
4. According to the Hartree-Fock method used in [14, 17], the atomic dispersion amplitudes f_a are calculated using a nonrelativistic form of wave equation, while the wave functions are presented as a product of the wave functions of separate electrons (a self-consistent field approach). On the contrary, the method by Cromer [18] employs the Dirac-Slater wave functions that take into account both the relativistic effects and the influence of normal and abnormal dispersion effects. As a matter of fact, our experimental values F_e^P, f_e^P and $\Delta f'^{,P}$ show a better agreement with the Cromer's theory.

Summing up, the comparison of the experimental and the calculated α and $\Delta f'$ parameters testifies that the normal and abnormal X-ray dispersions in our crystals are most completely described by the Cromer theory [18].

References

1. Kittel Ch, Introduction to solid state physics (Translated from English, Ed. Gusev A A). Moscow: Nauka (1978).
2. Aluker E D, Encyclopaedic dictionary "Solid state physics". Vol. 2 Kiev: Naukova Dumka (1998).
3. James R, Optical principles of X-ray diffraction (Translated from English, Ed. Iveronova V I). Moscow: Inostrannaya Literatura (1950).
4. Iveronova V I and Revkevich G P, Theory of X-ray dispersion. Moscow: Moscow State University (1972).
5. Raransky M D and Struk Ya M, Diffraction optics of X-rays. Chernivtsi: Ruta (2007).
6. Belomestnikh V N and Tesleva E P, 2004. Relationship of anharmonicity and lateral deformation of quasi-isotropic polycrystalline solids. Theor. J. Phys. **74**: 140–142.
7. Sanditov D S, Mantatov V V and Sanditov B D, 2009. Anharmonicity of lattice vibrations and transverse deformation of crystalline and vitreous solids. Phys. of the Sol. State. **51**: 998-1003.
8. Raransky M D, 1999. Normal and anomalous dispersion of X-ray waves. Sci. Bull. of Chernivtsi University, Ser. Physics. **57**: 5–11.
9. Raransky A M, Struk J M, Fodchuk I M. and Raransky M D, 1993. Solution of x-ray diffraction inverse problems in optics, Proc. SPIE. **2108**: 320-326.
10. Fodchuk I M and Raransky N D, 2003. Moire images simulation of strains in X-ray interferometry. J. Phys. D: Appl. Phys. **36**: 55–59.
11. Raransky M D, 2009. The phenomenon of pendular oscillations related to X-waves in real single crystals. Sci. Bull. of Chernivtsi University, Ser. Physics and Electronics. **438**: 11–19.

12. Raransky M D, Pendulum and Moiré fringes in real crystals. Doctoral Thesis in Physics and Mathematics. Chernivtsi (1987).
13. Mirkin L I, Handbook on X-ray diffraction analysis of polycrystals. Moscow: FML (1961).
14. International tables for X-ray crystallography (Ed. Lonsdale K) Birmingham: Kynoch Press (1972).
15. Doyle P A and Turner P S, 1968. Relativistic Hartree-Fock X-ray and electron scattering factors. Acta Cryst. A. **24**: 390–393.
16. Zachariasen W H, 1968. Extinction in a lithium fluoride sphere. Acta Cryst. A. **24**: 324–332.
17. Barnea Z, 1966. Hönl's anomalous dispersion corrections for atomic scattering factors. J. Phys. Soc. Japan. **21**: 961–963.
18. Cromer D T, 1965. Anomalous dispersion corrections computed from self-consistent field relativistic Dirac-Slater wave functions. Acta Cryst. **18**: 17–23.

Raransky M.D., Balazyuk V.N., Sergeev V.M. and Melnyk M.I., 2011. Optical parameters of CaF_2, LiF, NaCl and KCl single crystals in the X-ray spectral range Ukr.J.Phys.Opt. **12**: 45–53.

Анотація. *В роботі використані методи маятникових коливань та X - променевої інтерферометрії для вимірювання параметра F_{hkl}, дисперсії атомних амплітуд f_a, дисперсійних поправок $\Delta f'$ і одиничних декрементів показників заломлення α монокристалів CaF_2, LiF, NaCl і KCl.*